IOP Publishing
Journal of Physics D: Applied Physics
J. Phys. D: Appl. Phys. 50 (2017) 015002 (6pp)
doi:10.1088/1361-6463/50/1/015002

Tunable Curie temperature around room temperature and magnetocaloric effect in ternary Ce–Fe–B amorphous ribbons

Zhu-bai Li[1,3], **Le-le Zhang**[1,2], **Xue-feng Zhang**[1,2], **Yong-feng Li**[1,2], **Qian Zhao**[1,2], **Tong-yun Zhao**[1,3] **and Bao-gen Shen**[1,3]

[1] Key Laboratory of Integrated Exploitation of Bayan Obo Multi-Metal Resources, Inner Mongolia University of Science and Technology, Baotou 014010, People's Republic of China
[2] School of Science, Inner Mongolia University of Science and Technology, Baotou 014010, People's Republic of China
[3] State Key Laboratory for Magnetism, Institute of Physics, Chinese Academy of Sciences, Beijing 100190, People's Republic of China

E-mail: lzbgj@163.com

Received 7 July 2016, revised 5 October 2016
Accepted for publication 11 October 2016
Published 22 November 2016

Abstract

$Ce_{13-x}Fe_{81+x}B_6$ ($x = 0$, 0.5, 1, 1.5, and 2) amorphous magnets were prepared by melt-spinning method. These magnets are magnetically soft at low temperature, and undergo a second-order phase transition from ferromagnetic to paramagnetic state near room temperature with a broad temperature span. The phase-transition temperature is tunable by the variation of the Ce/Fe atomic ratio, which is mainly due to the change of the coordination number of Fe atoms in these ternary Ce–Fe–B amorphous magnets. Though the entropy change is low, the refrigeration capacities are in the ranges of 116–150 J kg^{-1} and 319–420 J kg^{-1}, respectively, for the magnetic field changes of 0–2 T and 0–5 T, which is comparable with those of conventional magnetic materials for room-temperature refrigeration. Given the low cost of Fe and Ce, Ce–Fe–B amorphous magnets are attractive magnetic refrigerant candidates.

Keywords: Ce–Fe–B, amorphous magnets, Curie temperature, magnetocaloric effect

S Online supplementary data available from stacks.iop.org/JPhysD/50/015002/mmedia

(Some figures may appear in colour only in the online journal)

1. Introduction

The change of magnetic entropy in magnetic materials is accompanied by an exothermic or endothermic process, which is regarded as a magnetocaloric effect and can be used for refrigeration [1–3]. Compared with conventional refrigeration, magnetic refrigeration is more energy-saving and environmentally friendly. The abrupt change of magnetization accompanied by the structural or volume transition leads to a large entropy change and large refrigeration capacity (RC) in first-order phase transition for crystalline magnets [4–7]. In amorphous magnets, the atomic arrangement is in long-range disorder, and so there is neither volume nor structural change accompanying the magnetic phase transition [8, 9]. Though their magnetization change is slow with a low entropy change in the second-order phase transition, amorphous magnets are also attractive for magnetic refrigerant applications due to their wide working temperature range, reduced magnetic hysteresis, and good mechanical properties [8, 9].

The Fe atom bears the largest magnetic moments per unit mass, which is desirable for obtaining large entropy change and refrigeration capacity, but Curie temperatures are much higher than room temperature in Fe-based amorphous alloys. The doping of refractory metals Nb, Zr, Ti, and Cr can not only tune Curie temperature but also improve the glass-forming ability [10–14]. Meanwhile, the saturation magnetization and RC are reduced due to the nonmagnetic element additions. Fe and rare-earth elements can form amorphous

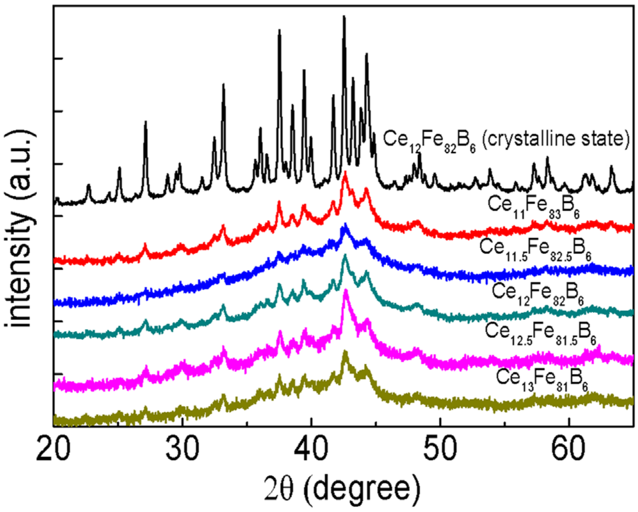

Figure 1. XRD patterns of Ce–Fe–B ribbons prepared by melt-spinning method with wheel-surface velocity of 50 m s^{-1}, and XRD pattern of $Ce_{12}Fe_{82}B_6$ crystalline ribbons prepared with low wheel-surface velocity of 20 m s^{-1}.

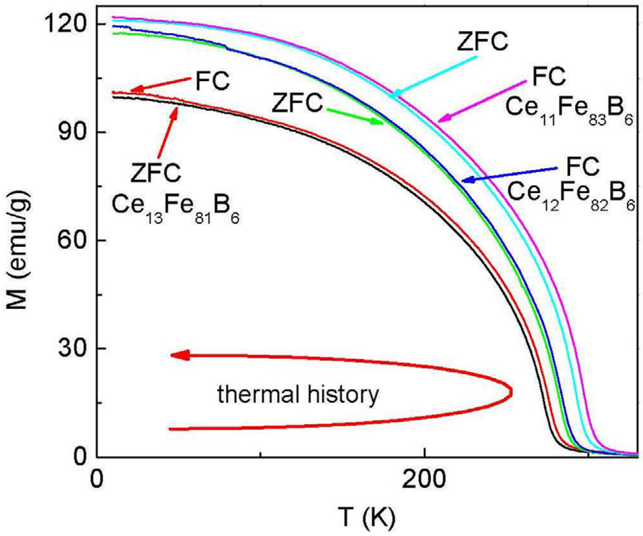

Figure 2. Temperature dependence of ZFC and FC magnetizations for Ce–Fe–B amorphous ribbons under a magnetic field of 0.02 T.

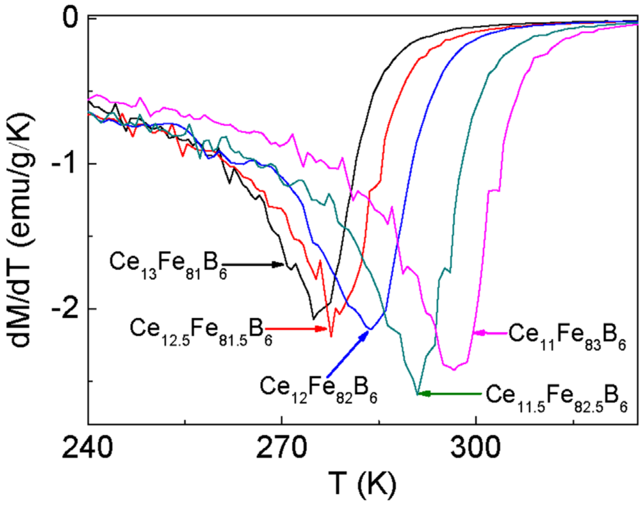

Figure 3. The derivative d*M*/d*T* versus *T* curves for Ce–Fe–B amorphous ribbons.

alloys, which can be used as magnetic refrigerants [15–18]. In this work, low-cost rare-earth Ce–Fe–B amorphous alloys are prepared by Ce, Fe, and FeB using a melt-spinning method. In these Ce–Fe–B magnets, the magnetocrystalline anisotropy is negligible at low temperature and the Curie temperature is around room temperature. The magnetic phase transition and magnetocaloric effect are systematically investigated in these ternary Ce–Fe–B amorphous magnets with the variation of Ce/Fe atomic ratio.

2. Experiment

The precursor ingots with nominal composition of $Ce_{13-x}Fe_{81+x}B_6$ ($x = 0, 0.5, 1, 1.5$, and 2) were produced from the mixture of high-purity Ce, Fe, and Fe–B alloys by arc-melting method under an argon gas. Melting was performed at least three times to ensure a good homogeneity of composition. An excess of 2wt.% for Ce was used to compensate the loss of volatilization during the melting process. The ribbons were obtained directly by induction-melting the precursor ingot and then ejecting the melt onto the surface of a rotating copper wheel with a surface velocity of 50 m s^{-1}. The x-ray diffraction (XRD) was used to check the phase constitution. Magnetic measurements were performed using a superconducting quantum interference device vibrating sample magnetometer with the field direction in the plane of the ribbons, and therefore the demagnetization factor was neglected.

3. Results and discussion

Figure 1 shows the XRD patterns of these ribbons. There exist much broadened diffraction peaks with weak intensity, which should be ascribed to the amorphous structure with atomic arrangement in short range order [16]. Since the angles of diffraction peaks correspond well to those of $Re_2Fe_{14}B$, there may be a small amount of nanocrystalline phase embedded in the amorphous matrix. For a comparison, the XRD pattern is also shown in figure 1 for $Ce_{12}Fe_{82}B_6$ ribbons prepared with low wheel-surface velocity of 20 m s^{-1}. The characteristic diffraction peaks are very strong, indicating long range order for atomic arrangement in crystalline structure. The atomic arrangement in amorphous structure may significantly affect the magnetic structure, which could be checked by the magnetization dependence on temperature. We first lowered the temperature to 10 K in the absence of an applied magnetic field. Then we increased the temperature from 10 K to 400 K under a field of 0.2 kOe and recorded the value of magnetic moments, which is called magnetization variation with temperature in zero-field cooling (ZFC). After that, we recorded the magnetization as the temperature decreased from 400 K to 10 K under a field of 0.2 kOe in field cooling (FC). As shown in figure 2, with the decrease of temperature the magnetization increases monotonously near room temperature, suggesting the occurrence of a magnetic phase transition from paramagnetic to

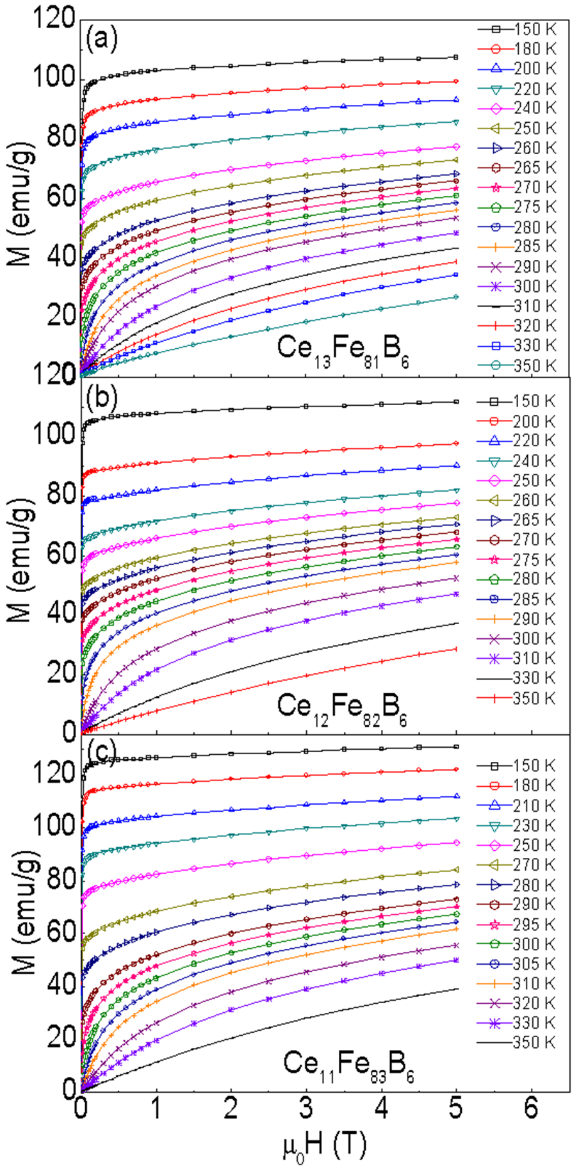

Figure 4. Magnetic isothermals in the temperature range of 150–350 K for $Ce_{13}Fe_{81}B_6$ (a), $Ce_{12}Fe_{82}B_6$ (b), and $Ce_{11}Fe_{83}B_6$ (c), respectively ribbons.

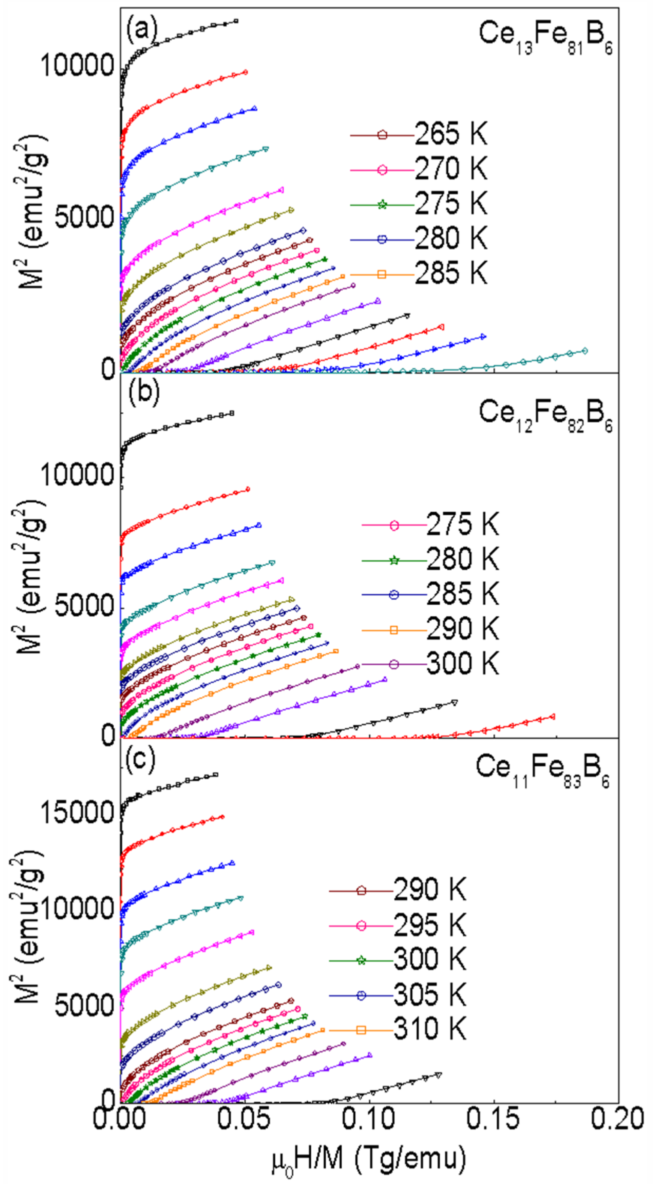

Figure 5. Arrott plots for the amorphous magnets of $Ce_{13}Fe_{81}B_6$ (a), $Ce_{12}Fe_{82}B_6$ (b), and $Ce_{11}Fe_{83}B_6$ (c), respectively.

ferromagnetic state [18, 19]. The slow increase in magnetization is attributed to the fluctuation of the exchange integral caused by the structural disorder in amorphous alloys [15, 20]. The curves of FC and ZFC nearly overlap in the whole temperature range, indicating negligible magnetic hysteresis and thermal hysteresis for these amorphous magnets. Curie temperature, determined by the maximum of dM/dT [8], is in the range between 270 K and 300 K (shown in figure 3), and is tunable by the variation of the Ce/Fe atomic ratio. The Curie temperature is about 460 K in Ce–Fe–B ribbons prepared with the copper surface velocity of 27 m s^{-1}, which is owing to the long-range order for atomic arrangement in the $Ce_2Fe_{14}B$ crystalline structure [21]. However, for the amorphous ribbons prepared with higher quenching rate, the phase-transition temperature decreases to room temperature.

Curie temperature is strongly dependent on the Fe–Fe atomic distance and coordination number [8, 10, 13, 22]. It has been argued that the number of surrounding Fe atoms for each Fe site plays a crucial role in determining T_C for Fe–B amorphous alloys [8, 13]. In these Ce–Fe–B amorphous magnets, the increase of Fe and the corresponding decrease of Ce atomic percent would lead to the increase of the coordination number Z_{Fe-Fe}. Hence, like the Fe–Zr and Fe–Ti alloys, it can be expected that the increase of the number of nearest neighbor Fe atoms is the origin of the systematic increase of T_C in these amorphous magnets [13, 22].

The phase transition is accompanied by an endothermic process, which depends on the entropy change from the magnetic ordering to disordering state. To determine the value of entropy change, the magnetization isotherms were measured under applied field up to 5 T. Figures 4(a)–(c) show the magnetization isotherms of $Ce_{13-x}Fe_{81+x}B_6$ amorphous ribbons for $x = 0$, 1, and 2, respectively. In rare-earth magnets the magnetic structure is complicated and includes helical

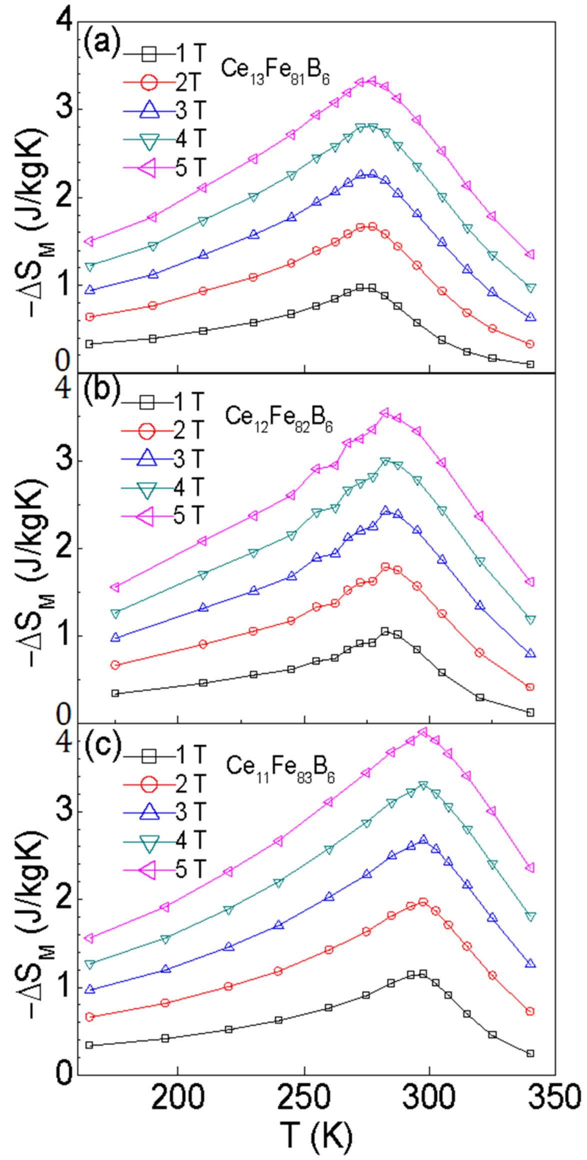

Figure 6. Temperature dependence of magnetic entropy changes for the Ce–Fe–B amorphous ribbons for different magnetic field changes up to 5 T.

structures and the spin configuration of the antiferromagnet. It can be seen that the magnetization reaches saturation quickly at the low temperature of 150 K, which is similar to that in the ferromagnet based on Gd in $Gd_{60}M_{30}In_{10}$ (M = Co, Ni, and Cu) at 5 K [15]. In spin glass alloys, it is hard to saturate even at the applied field of 5 T [10, 15, 19]. This fact verifies the ferromagnetic and excellent magnetically soft properties in these Ce–Fe–B amorphous magnets. Ce–Fe–B bears magnetocrystalline anisotropy of 26 kOe in a $Ce_2Fe_{14}B$ crystalline structure [23], but the anisotropy is negligible in an amorphous structure. It is also noted that the magnetization at 150 K for $Ce_{11}Fe_{83}B_6$ is greater than that of $Ce_{13}Fe_{81}B_6$ and $Ce_{12}Fe_{82}B_6$ ribbons, which should be attributed to the higher content of Fe in $Ce_{11}Fe_{83}B_6$ ribbons.

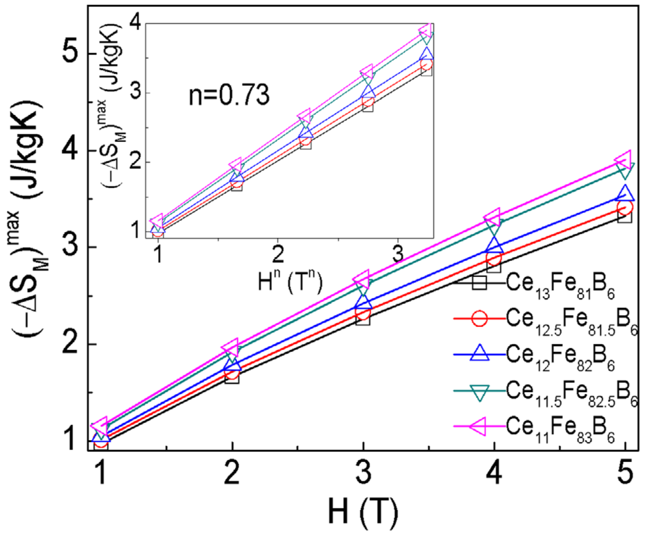

Figure 7. Dependence of the maximum magnetic entropy changes on magnetic field *H* for the Ce–Fe–B amorphous magnets. Inset shows fitting result of H^n.

To check the character of phase transition in the Ce–Fe–B amorphous magnets, the Arrott plots are shown in figures 5(a)–(c), which are derived from *M*–*H* isotherms. According to the Banerjee criterion [24], the positive slope on the Arrott curve confirms the typical characteristic of a second-order magnetic transition from the ferromagnetic to paramagnetic state. Based on the thermodynamic theory, the magnetic entropy change is calculated from the isothermal magnetization by the Maxwell relation, $\Delta S_M(T,H)=\int_0^H (\partial M/\partial T)_H \mathrm{d}H$ [25]. Figure 6 shows the temperature dependence of entropy change ($-\Delta S_M$) for different applied field changes. Compared with those of many crystal magnets, though the maximum of ($-\Delta S_M$) is smaller, a very broad distribution of ($-\Delta S_M$) is exhibited, indicating a wide temperature span which is desirable for an Ericson cycle magnetic refrigerator. The wide temperature span results from the slow magnetization change in the magnetic phase transition due to the disordered structure [8, 9]. The maximum of the entropy change ($-\Delta S_M$) for a field change of 0–5 T increases from 3.3 to 3.9 J kg^{-1} K, with *x* increasing from 0 to 2 in $Ce_{13-x}Fe_{81+x}B_6$. The increase of Fe content would lead to an increase of saturation magnetization and a large change of magnetization in magnetic phase transition, which should be ascribed to the variation of entropy change ($-\Delta S_M$) with the Ce/Fe atomic ratio. With the increase of Fe content, the corresponding position of the maximum of ($-\Delta S_M$) shifts to higher temperature. This fact is consistent with the variation of Curie temperature with Ce/Fe atomic ratio, indicating the tunable working temperature for magnetic refrigeration in these Ce–Fe–B amorphous magnets.

For the second-order magnetic phase transition, the field dependence of the maximum magnetic entropy change can be expressed as $(-\Delta S_M) \propto H^n$ based on the mean field theory [26, 27]. The relations of ($-\Delta S_M$) maximum and *H* are shown in figure 7. As shown in the fitting figure plotted in the inset, the value of *n* is 0.73, which is consistent with the results for Fe-based amorphous alloys [27] but higher than the theoretical value 2/3 for mean field theory. Possibly it is the failure of the mean field picture for these second-order phase-transition materials [28]. In addition, the value of *n* is also affected by

Table 1. Magnetocaloric properties of different magnets for room-temperature refrigeration. A and C represent amorphous and crystalline structures, respectively.

Sample (Structure)	T_C (K)	$(-\Delta S_M)$ (0–2 T) ($J\ kg^{-1}\ K^{-1}$)	$(-\Delta S_M)$ (0–5 T) ($J\ kg^{-1}\ K^{-1}$)	RC (0–5 T) ($J\ kg^{-1}$)	Refs.
$Ce_{13}Fe_{81}B_6$ (A)	275	1.66	3.32	319.3	This work
$Ce_{12.5}Fe_{80.5}B_6$ (A)	278	1.71	3.41	348.13	This work
$Ce_{12}Fe_{80}B_6$ (A)	284	1.78	3.54	353.27	This work
$Ce_{11.5}Fe_{79.5}B_6$ (A)	291	1.91	3.81	409.76	This work
$Ce_{11}Fe_{79}B_6$ (A)	297	1.96	3.90	420.09	This work
$La_{0.8}Ce_{0.2}Fe_{11.5}Si_{1.5}C_{0.4}$ (C)	246	7.6	13.5	330	[30]
$Gd_5Ge_2Si_2$ (C)	280		19.2	200	[31]
$MnFeP_{0.45}As_{0.35}$ (C)	300	14.5	18	225	[6,33]
$Fe_{66.3}V_{13.7}B_{12}Si_8$ (A)	335	1.034			[8]
$Fe_{83}Nd_5Cr_8B_4$ (A)	322	1.8	3.4		[34]

the structural inhomogeneity due to the free volume, atomic cluster, and even nano-crystallized grains embedded in the disordered matrix [29].

In the refrigeration cycle, accompanied by the entropy change, the working material absorbs the heat from the load and the RC can be quantified by the heat absorbed per kilogram [9]. As suggested by Wood and Potter [30], RC is determined by the integral $\mathrm{RC} = \int_{T_{\mathrm{cold}}}^{T_{\mathrm{hot}}} \Delta S_{(T,\Delta H)} \mathrm{d}T$. Here, T_{hot} and T_{cold} are defined as the temperature boundary at the hot and cold ends, respectively, corresponding to the half maximum of $(-\Delta S_M)$ on the $(-\Delta S_M) - T$ curve. The values of RC for Ce–Fe–B amorphous magnets are 117–150 J kg^{-1} and 319–420 J kg^{-1}, respectively, for magnetic field changes of 0–2 T and 0–5 T, which are larger than those of most amorphous alloys with T_C near room temperature. Though possessing small magnetic entropy change, their RCs (for magnetic field change 0–5 T) are also higher than those of most crystalline materials for room-temperature refrigeration, such as $La_{0.8}Ce_{0.2}Fe_{11.5}Si_{1.5}C_{0.4}$ (330 J kg^{-1}) [31], $Gd_5Ge_2Si_2$ (200 J kg^{-1}) [32], and $MnFeP_{0.45}As_{0.35}$ (225 J kg^{-1}) [6, 33]—though, of course, considering the too-large temperature span, the real refrigerant capacity may be reduced more or less in practical technology for these amorphous magnets. Fe bears the largest magnetic moments per kilogram among the magnetic elements. The high RC should be attributed to the higher content of the magnetic element Fe with fewer amounts of nonmagnetic elements as well as the amorphous structure. Table 1 lists the magnetic properties (the values of T_C, $(-\Delta S_M)$, and RC) for some typical magnets as well as Ce–Fe–B amorphous magnets for room-temperature refrigeration. Ce is cheap and the most abundant of rare earth resources and overstocked due to the overconsumption of Nd and Pr elements [23]. Combining the particular merits coming from their amorphous nature and large RC, Ce–Fe–B amorphous magnets are also attractive candidates for use as magnetic refrigerants in room-temperature refrigeration.

4. Conclusions

In summary, ternary Ce–Fe–B amorphous magnets can be prepared by the melt-spin method with higher quenching rate. Compared to Ce–Fe–B crystalline magnets, the Curie temperature in these amorphous magnets decreases to room temperature and magnetocrystalline anisotropy is negligible at low temperature. The working temperature range is wide, and the magnetic as well as thermal hysteresis is negligible due to the disordered atomic arrangement. The entropy change that accompanies the magnetic phase transition is larger than those of most amorphous magnets for room-temperature refrigeration, which should be attributed to the higher content of the magnetic element Fe and lower content of the nonmagnetic elements. The values of RC for Ce–Fe–B amorphous magnets are 117–150 J kg^{-1} and 319–420 J kg^{-1}, respectively, for magnetic field changes of 0–2 T and 0–5 T, which are larger than those of most amorphous alloys with T_C near room temperature. Due to the considerable refrigeration capacity, low cost Ce–Fe–B magnets are also attractive candidates for use as magnetic refrigerants in room-temperature refrigeration.

Acknowledgments

The present work was supported by the National Basic Research Program of China (Grant No. 2014CB643702) and the National Natural Science Foundation of China (Grant Nos. 51461033, 11274357, 51590880).

References

[1] Gschneidner K A Jr, Pecharsky V K and Tsokol A O 2005 *Rep. Prog. Phys.* **68** 1479
[2] Brück E 2005 *J. Phys. D: Appl. Phys.* **38** R381
[3] Shen B G, Hu F X, Dong Q Y and Sun J R 2013 *Chin. Phys.* B **22** 017502
[4] Pecharsky V K and Gschneidner K A Jr 1997 *Phys. Rev. Lett.* **78** 4494
[5] Hu F X, Shen B G, Sun J R, Cheng Z H, Rao G H and Zhang X X 2001 *Appl. Phys. Lett.* **78** 3675
[6] Tegus O, Brück E, Buschow K H J and De Boer F R 2002 *Nature* **415** 150
[7] Hu F X, Shen B G and Sun J R 2013 *Chin. Phys.* B **22** 037505
[8] Boutahar A, Ettayfi A, Alouhmy G, Lassri H, Hlil E K, and Fruchart D 2014 *J. Supercond. Nov. Magn.* **27** 2401
[9] Caballero-Flores R, Franco V, Conde A, Knipling K E and Willard M A 2010 *Appl. Phys. Lett.* **96** 182506
[10] Kiss L F, Kemény T, Franco V and Conde A 2015 *J. Alloys Compd.* **622** 756

[11] Tian H C, Zhong X C, Liu Z W, Zheng Z G and Min J X 2015 *Mater. Lett.* **138** 64

[12] Law J Y, Franco V and Ramanujan R V 2011 *Appl. Phys. Lett.* **98** 192503

[13] Waske A, Schwarz B, Mattern N and Eckert J 2013 *J. Magn. Magn. Mater.* **329** 101

[14] Zhang H Y, Li R, Xu T, Liu F M and Zhang T 2013 *J. Magn. Magn. Mater.* **347** 131

[15] Mayer C, Gorsse S, Ballon G, Caballero-Flores R, Franco V and Chevalier B 2011 *J. Appl. Phys.* **110** 053920

[16] Yuan F, Li Q and Shen B L 2012 *J. Appl. Phys.* **111** 07A937

[17] Law J Y, Ramanujan R V and Franco V 2010 *J. Alloys Compd.* **508** 14

[18] Dong Q Y, Shen B G, Chen J, Shen J, Wang F, Zhang H W and Sun J R 2009 *J. Appl. Phys.* **105** 053908

[19] Wang F, Shen J, Zhang J, Sun J R and Shen B G 2009 *J. Appl. Phys.* **105** 07A944

[20] Liu X Y, Barclay J A, Gopal R B, Földeàki M, Chahine R, Bose T K, Schurer P J and LaCombe J L 1996 *J. Appl. Phys.* **79** 1630

[21] Li Z B, Shen B G, Zhang M, Hu F X and Sun J R 2015 *J. Alloys Compd.* **628** 325

[22] Fukamichi K and Satoh Y 1985 *IEEE Transl. J. Magn. Japan* **9** 1101

[23] Li Z B, Zhang M, Shen B G, Hu F X and Sun J R 2016 *Mater. Lett.* **172** 102

[24] Banerjee B K 1964 *Phys. Lett.* **12** 16

[25] Shen J, Zhao J L, Hu F X, Rao G H, Liu G Y, Wu J F, Li Y X, Sun J R and Shen B G 2010 *Appl. Phys.* A **99** 853

[26] Oesterreicher H and Parker F T 1984 *J. Appl. Phys.* **55** 4334

[27] Franco V, Blázquez J S and Conde A 2006 *Appl. Phys. Lett.* **89** 222512

[28] Zhong X C, Huang X W, Shen X Y, Mo H Y and Liu Z W 2016 *J. Alloys Compd.* **682** 476

[29] Liu G L, Zhao D Q, Bai H Y, Wang W H and Pan M X 2016 *J. Phys. D: Appl. Phys.* **49** 055004

[30] Wood M E and Potter W H 1985 *Cryogenics* **25** 667

[31] Zhang H, Shen J, Xu Z Y, Zheng X Q, Hu F X, Sun J R and Shen B G 2012 *J. Magn. Magn. Mater.* **324** 484

[32] Provenzano V, Shapiro A J and Shull R D 2004 *Nature* **429** 853

[33] Johnson F and Shull R D 2006 *J. Appl. Phys.* **99** 08K909

[34] Lai J W, Zheng Z G, Zhong X C, Franco V, Montemayor R, Liu Z W and Zeng D C 2015 *J. Magn. Magn. Mater.* **390** 87